Global Distribution of Superbolts

By

R. H. Holzworth[1], M.P. McCarthy[1], J. B. Brundell[2], A. R. Jacobson[1] and C. J. Rodger[2]

5/8/19 (Revised 7/18/19)

1. Earth and Space Sciences, University of Washington, Seattle, WA, USA
2. Department of Physics, University of Otago, Dunedin, New Zealand

Key Points:

1. Superbolts, with more than 10^6 Joules of radiated VLF energy/stroke between 7 and 18 kHz are identified using WWLLN (World Wide Lightning Location Network) data during a nine year study of more than $2x10^9$ global lightning strokes. These Superbolt energies are more than three orders of magnitude above the mean energy of the total global distribution.
2. Superbolts occur predominantly during November – February months with peak occurrence regions in the eastern North Atlantic, Mediterranean Sea and over the Andes mountains, with smaller densities in the North Pacific east of Japan, in the equatorial Atlantic and Indian oceans and south of S. Africa. The superbolt distribution does not show peaks over the main total lightning regions of the Americas, Africa and the Maritime Continent.
3. One to one stroke comparisons with the Earth Networks Total Lightning Network show that all superbolts have peak currents over 10^5 Amps

Abstract: We use World Wide Lightning Location (WWLLN) data on the radiated radio frequency electromagnetic energy per stroke to identify the upper tip of the global lightning stroke energy distribution. The mean stroke energy is about 1000 Joules/stroke in the VLF band between 5 and 18 kHz while the distribution used in this paper is limited to strokes in that band above 1 MJ, about three orders of magnitude above the mean. It is shown that these energies are representative of the tip of the optical distribution, first identified by Turman (1977) above 10 GW/stroke which he termed 'Superbolts'. The distribution peaks globally in the northern hemisphere winter (November – February) with most superbolts being found in the North Atlantic west of Europe, the winter Mediterranean Sea, and a strong local maximum over the Andes in South America. We identify regions with somewhat fewer superbolts in the North Pacific east of Japan in winter, along the equator of the Atlantic and Indian Oceans and south of South Africa. We find very few superbolts during April – October each year. While superbolts are scattered around the globe, the local occurrence peaks do not coincide with the usual three main lightning 'chimneys'. Unlike the distribution of all normal global lightning, we find superbolts predominantly over the oceans and seas, with fewer over the continents, just the opposite of all global lightning.

Introduction

We have examined nine years of WWLLN data which includes $2*10^9$ located lightning strokes for the years 2010 – 2018 in a parameter study of geolocation and energy per stroke. From this data set we have focused on strokes with energy/stroke about three orders of magnitude above the mean energy (which itself is very close to the median energy of about 10^3 Joules of far-field radiated electromagnetic energy in the frequency band from 5 to 18 kHz as described in Hutchins

et al 2012a and to be shown here). The far-field, radiated VLF energy-per-stroke estimated by WWLLN includes all the VLF radiation propagated within the Earth-ionosphere waveguide in the frequency band of 5 to 18 kHz. That is, the estimated energy includes only that portion whose initial departure rays (from the source stroke) are grazing-incidence at the underside of the ionospheric D-layer. Only the grazing-incidence portion is capable of populating low-order waveguide modes that can propagate with low attenuation and can be detected at distances > 5000 km. Moreover, the steep incidence remainder of these sferics is mostly lost to joule heating in the ionosphere above the stroke. Here we identify this top part of the energy/stroke distribution with the 'superbolts' identified and defined by Turman, 1977. Turman used optical stroke data obtained by the Vela satellites to identify the top range of source stroke optical energies which were '100 times more intense than the typical lightning'. Turman 1977 found about 20 strokes in the Vela data set in the superbolt category at locations all around the globe, and noticed that a large number of them were seen in the winter hemisphere near Japan and across to the eastern north Pacific Ocean.

In a follow up study using optical flash data from the Forte satellite, Kirkland (1999) found 2735 superbolts, out of 600,000 lighting events (0.46%) catalogued by the satellite. Although the strokes studied by Turman (1977) or by Kirkland (1999) could not be accurately geolocated with just a photodiode, Kirkland did present a global of map of the low earth orbit satellite subtrack at the times of superbolt detection. His distribution supports the notion that superbolts can occur anywhere, and in particular he identified the three main thunderstorm 'chimney' regions (Americas, Africa and Maritime continents) as the principle areas for most superbolts. He did not suggest that his work had agreed with Turman about finding an enhanced likelihood of superbolts in the north Pacific winter hemisphere east of Japan. Indeed, Kirkland's distribution

of energetic strokes from the FORTE satellite represented 0.004 of his total strokes, while the WWLLN energetic strokes studied here represent a much smaller fraction (0.00004) of strokes with energies at the very tip of the total distribution (shown in the next section).

In this work we will describe our methodology, which differs from both the Vela and Forte studies, in that the WWLLN lightning location network determines stroke locations using radio frequency methods, not optical. Additionally, WWLLN measures the average energy/stroke (proportional to the integral of E^2 through the sferic), and not the peak power, while the optical studies used peak optical power to categorize the strokes. We will use our full energy distributions to choose those strokes over 10^6J, which are three orders of magnitude above the mean stroke energy. Then we compare these strokes to the optically determined superbolt properties. Our conclusions will show that, while some superbolts are seen originating in the three usual thunderstorm 'chimneys', nevertheless most superbolts can be grouped into a small number of regions mostly over water and not coincident with the chimneys. One of the regions with superbolts we identify is that area east of Japan in the North Pacific winter, also seen by Turman 1977. We also identify a few other regions not near the usual chimneys. Indeed the preponderance of superbolts occur in the northern hemisphere winter hemisphere as we will show.

By way of corroborating our superbolt data with other networks, we compare one-to-one stroke locations reported by the ENTLN (Earth Networks Total Lightning Network) showing that the superbolt distribution found by WWLLN corresponds to very high peak current events in the ENTLN data set as well. In addition we present one waveform example of a superbolt sferic to show the signals are well resolved at multiple WWLLN receivers from a few thousand km distance, to nearly half way around the world.

92 **Data used in this Study**

93 The WWLLN lightning location network grew out of the TOGA network (see Dowden et al
94 2002) and has been globally operational since August 2004. Many previous papers have
95 described the network and multiple scientific results derived from it (Lay et al, 2004, Rodger et
96 al, 2006, Jacobson et al, 2006, Price et al, 2007, Connaughton et al, 2010, Abarca et al, 2010,
97 Hutchins et al, 2012a and 2012b, Virts et al, 2013, Thornton et al, 2017).
98 A brief summary of the methodology of the WWLLN network is as follows. WWLLN currently
99 uses over 80 stations distributed globally to detect Very Low Frequency (VLF) radiation in the
100 band from 100 Hz to 24 kHz sampled at 48,000 samples/sec or faster to identify lightning
101 transients. These receiving stations process each sferic wave packet to determine the time of
102 group arrival (TOGA) (see Dowden et al, 2002). These TOGA times, accurate to about a
103 microsecond, from 5 or more WWLLN stations are used to determine the source location in a
104 global time-of-arrival analysis. Rodger et al (2006) showed that each WWLLN station can
105 identify strokes out to about 6,000 km in the daytime and out to 10 to 12,000 km at night.
106 Indeed, they showed that the larger the peak current of the stroke (as identified by the New
107 Zealand Lightning Detection Network) the more likely it was for more WWLLN stations to
108 detect the stroke, and to participate in the location determination. In a recent follow up to
109 Rodger et al, 2006 the detection efficiency of WWLLN for strokes above 50 kA peak current is
110 now up to about 80% by comparison to NZLDN network data as shown in Figure 1. This figure
111 shows the evolution of the WWLLN detection efficiency as a function of peak current seen by
112 the NZLDN lightning network, and explained by Rodger et al, 2006 (see Fig 5 in that paper).
113 For the years of this study, WWLLN has highest detection efficiency, at 60--80%, for large
114 amplitude strokes.

115 For completeness, it is worth noting two points about detection efficiency. First we note that the
116 global annual total of WWLLN strokes increased by 68% over the test period, with most of that
117 increase before 2014 (64%) then some variations up and down after that by a few percent.
118 (see Table 1). So, the network performance in terms of individual stroke detections increased by
119 almost an order of magnitude over the test period, with most of that increase in the first few
120 years, then a leveling off with a few percent change in each of the later few years.
121 Additionally, it is important to understand how WWLLN detection efficiency varies from place
122 to place around the world and with time. Hutchins et al (2012b) developed a method to correct
123 for relative detection efficiency variations. WWLLN routinely publishes the hourly, global
124 relative detection efficiency on a 1^{o} x 1^{o} global grid (see http://wwlln.net/deMaps) whereby the
125 stroke density at any location can be compared to that of any other region. After these
126 corrections are applied, the WWLLN data can be compared around the world as if WWLLN had
127 nearly constant detection efficiency everywhere. As time has marched on these 'correction
128 factors' have come closer to 1.0 for nearly all global locations (typically ranging from .90 to .99)
129 so these relative detection efficiency corrections have little effect on the overall WWLLN data
130 set anymore. The point here is that WWLLN has relatively smooth detection efficiency on a
131 daily basis all around the world. Of course, these studies were done with the whole WWLLN
132 data set, and not just the high energy population being studied here. So, below we talk further
133 about verifying the data set with one to one comparisons to other networks.
134
135 The present work was enabled in part by the work of Hutchins et al (2012a) in which they
136 developed a method to calculate the energy/stroke for each WWLLN stroke. In April 2009 the
137 WWLLN network started saving the necessary data, involving an integration of the

138 electromagnetic field squared during each sferic interval. With the calibrated electric field
139 squared (E^2) at each antenna, together with the VLF attenuation from the stroke source to that
140 station using the US Navy LWPC code (Long Wavelength Propagation Capability, see
141 Thompson 2010) we obtain the source energy/stroke. The present study uses the energy/stroke
142 from all of 2010-2018 for each located lightning stroke (about $2*10^9$ strokes during the 9 year
143 data set).
144
145 Hutchins et al (2012a) demonstrated that the global distribution of stroke energies was log
146 normal in shape, such as shown for the current data set in Figure 2. In this Figure we present the
147 log of the energy versus the log of the histogram distribution for this entire 9 year WWLLN data
148 set. The histogram of energies is approximately log normal as expected, with the mean and
149 median near 1000 J. Hutchins showed that the peak for any given subset in time and space can
150 vary around between about 400 J to 2500 J but was very consistently within this range for the
151 years of their initial study (2009 – 2012) and agrees well with the current data shown in Figure 2.
152 Indeed, here we find the global energy distribution is still in this range with the mean and median
153 near 10^3 J as for the years studied by Hutchins et al (2012a).
154 As mentioned above, the data set we are using has more than 10^9 strokes, which we have
155 examined entirely for large amplitude strokes (above 10^6 J, shown in brown shading in Figure 2).
156 To ensure our sample of large strokes is not contaminated by erroneous data, we also make these
157 cuts in the data: the standard error of the energy fit is less than 30% of the energy for that stroke,
158 and at least 7 WWLLN stations detect the stroke. Rodger et al (2006) showed that there is a
159 strong relation between the peak current and the number of WWLLN stations detecting a stroke.
160 Hutchins et al 2012a showed that there is a monotonic relation between peak current and stroke

161 energy. Thus using 7 or more stations required for inclusion in this study does not limit the
162 range of high energy strokes, but it does eliminate strokes which might have poor energy
163 determination from too few stations involved. Nevertheless, it is clear from Figure 2 that the
164 high energy part of the distribution used in this study (brown shading) is a continuation of the
165 entire global energy distribution representing the upper tip of the log normal energy distribution.
166 After the next section discussing the overall WWLLN detection efficiency, we will then
167 concentrate on this upper part of the energy distribution to examine the most energetic strokes.
168 This upper part of the distribution includes 8,171 strokes with energy above 10^6 J which also
169 meet our selection criteria described above. These ~10^4 strokes amount to just a tiny percentage
170 of all the WWLLN strokes (~10^9 strokes) during the nine years of this study (as identified in
171 Figure 2 at the upper end of the overall energy distribution.) The strong cuts to the working
172 distribution (requiring 7 or more station and relatively small energy errors), provide us a very
173 clean distribution for spatial and temporal analysis.
174
175 **WWLLN Lightning Stroke Detection Efficiency**
176 As the WWLLN network has grown, so has the detection efficiency (DE) (see Rodger et al,
177 2006). Just before the data used in this study, Abarca et al, 2010 compared the detection
178 efficiency of WWLLN with the US National Lightning Detection Network, finding that
179 WWLLN, with its 28 to 38 global stations at the time, was detecting 10.3% of all cloud to
180 ground strokes, and 4.8% of all In Cloud strokes. Also at about this time, Abreu et al, 2010
181 found similar WWLLN DE for 2008 as compared to the Canadian Lightning Detection Network
182 (CLDN) near Toronto, and noted that the WWLLN DE for strokes with peak current above 50
183 kA was over 50%, similar to the New Zealand data in Figure 1 for that year. As the WWLLN

network grew from 2010 – 2018 the total number of located strokes rose from 139 million in 2010 to 233 million in 2018 (see table 1), a 67% increase over the course of this study. In the Rudlosky and Shea (2013) paper, where WWLLN and TRMM/LIS data are compared for 2009-2012 flashes, they found similar DE of 9.2% in 2012 and noted that WWLLN DE increased to 17.3% over water compared to land at 6.4%. A study comparing WWLLN DE to TRMM/LIS in the middle of the data period for this study (that is, between 2012-2014) was done by Burgesser 2017 in which he compared WWLLN strokes to TRMM/LIS flashes, and found that more than one stroke located by WWLLN occurred during a TRMM/LIS flash, for a 1.5 times multiplicity, meaning essentially all TRMM/LIS flashes were detected by WWLLN while about 70% of WWLLN strokes in the TRMM/LIS field of view were detected by TRMM/LIS, which Burgsser noted was below the DE expected for the TRMM/LIS instrument.

These studies, comparing to both ground based and space-borne lightning detectors, suggest that during this study of superbolts the DE of strong lightning strokes by WWLLN ranged from about 50% to over 80% of all strokes with peak currents greater than 50 kA. Furthermore the WWLLN DE is likely to be greatest over the oceans by a factor of 2 to 3 compared to the DE over land.

Verifying the data set.

The use of WWLLN far-field radiated energy values as a way to identify the source energy in the VLF range has been demonstrated in several previous papers (Hutchins et al, 2012a,b, 2013, Burkholder et al, 2013). However, since we are focusing this paper on a particular subset of the WWLLN energy distribution (above 10^6 J), we verify that these are high energy strokes using other data. First we compare to samples from the Earth Networks lightning location data where peak current is determined for strokes that have been identified by both the ENTLN (Earth Networks Total Lightning Network) and by WWLLN. As we will see, most of the high energy

strokes we report here are not found in regions where the ENTLN network has good coverage. However we did find some overlap. Table 2 gives some examples for all the large strokes in this study which occurred in the Continental USA (CONUS) where ENTLN has good coverage. We found 15 large energy strokes (>10^6 J) in the region and for every one we also found that ENTLN had located the stroke (i.e. 100% of WWLLN superbolts in the CONUS were also located by ENTLN). These large amplitude strokes are all classified as cloud to ground strokes by ENTLN and include both positive and negative polarity strokes. Figure 3a gives the average peak current distribution for ENTLN (from Hutchins et al, 2012c) for the CONUS in 2011 showing that the mean peak current for negative strokes was about -13 kA, while in Figure 3b we give the distribution for these 15 matched samples of large peak current (large WWLLN energy) strokes. We note that the mean peak current of the large negative matched strokes (here called superbolts) is -267 kA which is 20 times the mean peak current in Figure 3a.

Another way to check these large strokes is to examine the received waveforms at multiple WWLLN stations. Unfortunately, the WWLLN network does not save the VLF waveforms for more than a few days because of limitations of both station-to-internet bandwidth, and local station disk space. So, when conducting this analysis (done in 2019) the waveforms for these 8171 strokes have been written over. Therefore we set up a few days of waveform capture from several WWLLN stations during January 2019 to look at a few sample superbolt waveforms. Figure 4 is an example of a WWLLN stroke located with 27 WWLLN stations (that is, seen by 27 separate stations!), where we captured the waveforms at 5 of those stations with stroke-station distances from 5786 km to 16667 km. The amplitudes in this multipanel Figure 4 are given in dimensionless values related to the voltage on the antennas and the gain factor, different at each

231 receiving station. To determine the radiated VLF energy at the source requires a daily full
232 network amplitude calibration along with an estimation of the attenuation during propagation
233 (using the US Navy Long Wavelength Propagation Code as described by Hutchins et al, 2012a).
234 Daily calibration is needed because the individual station gain settings can and do change when
235 stations are adjusted for performance optimization. The characteristics of these plots in Figure 4
236 demonstrate that these large amplitude strokes are high quality VLF sferic wavepackets, which
237 stick out above all local system noise, even for stations nearly at the antipode. This is further
238 evidence that the large stroke data set is composed of strokes which look just like all normal
239 VLF sferics.
240
241 **Global Distribution**
242 So far we have identified, and provided examples and distributions, of the energy of these large
243 amplitude lightning sferics from the WWLLN data set. Here we discuss the global distribution
244 of these superbolts. Figure 5 presents a global plot of all 8171 large strokes broken into two
245 colors by energy. Blue dots are for strokes with energy between 10^6 J and $2*10^6$ J and the red
246 dots are for the strokes above $2*10^6$ J. From Figure 5 we can see that the global distribution of
247 these large strokes does not resemble the usual global lightning distribution such as shown by
248 Virts et al (2013). The global distribution of all lightning is well known to have about 10 times
249 more strokes over continents than over the oceans (c.f. Lay et al, 2007). Furthermore the major
250 regions of lightning generation, often referred to as the 'three chimneys' occur for the tropical
251 and subtropical regions of the Americas, Africa and the Maritime continent. None of these three
252 chimneys is well populated by superbolts in Figure 5. In figure 5 we notice that indeed, there are
253 some strokes over all continents but the three most dominant superbolt regions are in the eastern

North Atlantic, the Mediterranean and over the Andes Mountains in S. America. In addition there are identifiable regions with superbolts extending from Japan out across the north Pacific Ocean, along the equatorial regions over the Atlantic and Indian Oceans and in the Southern Ocean near South Africa.

Figure 6 presents just the red strokes (energy > $2*10^6$ J) given in Figure 5, which helps identify the peak superbolt occurrence regions. A subset of the data plotted in Figure 6 is enhanced in Figure 7 showing the eastern North Atlantic over to, and including the Mediterranean Sea. Here in Figure 7 we notice how clearly the superbolts outline the Eastern European coast line, as well as that of Italy in the Mediterranean (note that even the Adriatic Sea is well populated with superbolts, while central Italy is nearly devoid.)

Now we present the seasonal variation of these superbolts in Figure 8. Here we see that there are 20 times more superbolts in December and January than there are for instance, in July. Looking at the whole year, we find 76% of all superbolts in the months Nov, Dec, Jan and Feb.

Since we have no clear theory about the cause of superbolts it is fair to ask the question of whether WWLLN has a seasonal bias in detection efficiency between northern hemisphere winter and summer times. So, we looked for any difference in the mean and median of the full WWLLN energy distributions between these two near-solstice seasons. Figure 9 shows a histogram of monthly number of superbolts through this study along with a plot of the log10 of the seasonal WWLLN mean energy for Dec-Jan compared to the mean energy of June-July each year. Again, as with Figure 8 there is a marked annual variation with many more superbolts in Dec-Jan than in June-July each year. The line plot in Figure 9 below the histogram shows the mean energy of the whole WWLLN distribution (discussed above to typically be around 1000 J, or 3.0 in log10 space). In this Figure 9 we can see that the strong annual superbolt count

277 difference cannot be attributed to simultaneous large seasonal changes in the WWLLN energy
278 calculation. So, we can rule out attributing the seasonality of the distribution to some kind of
279 overall shift in the average energies. Indeed, the season with the highest mean energy (June-July
280 2014) corresponds to a minimum in superbolts, not a maximum, as one might expect if the whole
281 energy distribution was shifted slightly higher.
282 To see how the absence of the three main global lightning 'chimneys' affects the total
283 distribution, we look just at global Superbolts during the four northern hemisphere winter months
284 in Figure 10. What is interesting here is that this Figure 10 (northern winter only with energy >
285 $2*10^6$ J) is almost the same as Figure 7 (all superbolts with energy > $2*10^6$ J in the study).
286 Taken together with Figure 8, the monthly distribution, we can summarize the data by noting that
287 the previously identified three largest superbolt regions (Northeast Winter Atlantic Ocean,
288 Winter Mediterranean Sea and over the Andes during Northern Winter (i.e. during Summer in
289 Chile, Bolivia and Peru) all occur during Nov – Feb months yearly. Other notable regions with
290 many superbolts are also present including the superbolts east of Japan across the North Pacific
291 in winter, as well as the two near equatorial regions in the Atlantic and Indian Oceans. The
292 enhanced region noted before located near South Africa is now missing (in northern winter).
293
294 **Discussion**.
295 We have presented details of a high energy stroke subset of the $2x10^9$ WWLLN strokes for 2010
296 – 2018. After several cuts in the data to eliminate possible poorly located or characterized
297 strokes, we identified a subset of over 8,000 strokes with radiated VLF energy over 10^6 Joules.
298 These strokes have energies more than 3 orders of magnitude above the mean (or median) of the
299 full distribution. We suggest that these strokes are part of the previously identified energetic

300 stroke distribution called Superbolts by Turman in 1977 using optical data from the Vela
301 satellite. Turman did not have good geolocation (his instrument viewed the entire spherical earth
302 from the satellite altitude) but he did identify an excess of superbolts east of Japan in the winter
303 north Pacific. Turman's superbolts were 2 orders of magnitude larger than the average of the
304 peak power of strokes detected by Vela. He figured superbolts were on the order of 10^{10} W to
305 10^{12} W of total optical power. Without a current experimental comparison of optical power with
306 radiated VLF energy, we cannot here confirm that the superbolts we identify in this study do,
307 actually correspond with the power of Turman's superbolts. However, since we are only looking
308 at the top 1/thousandths of a percent of all the WWLLN strokes, which have energies three
309 orders of magnitude above the mean and median, we argue here that these WWLLN superbolts
310 are in or above the same power range as Turman identified from optical measurements. Now
311 that the Geostationary Lightning Mappers (GLM from GOES-16 and GOES-17) are operational,
312 perhaps we can do some one to one comparisons during next northern hemisphere winter. We
313 do not know the physical origins of these powerful strokes, nor whether they cause more
314 destructive ground strikes. It is also not known if their exceptional strength is matched by
315 exceptional effects in the overhead ionosphere, but we can suggest some possible avenues for
316 further work.
317 The superbolt properties this paper reports includes:
318 1. Energy distribution appears as a smooth continuation of the total WWLLN stroke energy
319 distribution (just the high energy tail)
320 2. Strong predominance of superbolts to occur over water
321 3. Very sharp contrast in occurrence at the coastlines
322 4. Strong occurrence maximum in December-January (northern winter)

5. Global distribution has no resemblance to the usual three lightning chimneys

6. The most dense superbolt regions include:

    a. north eastern North Atlantic from -20° Longitude to the European coastlines, and from Spain to mid-Norway
    b. Mediterranean Sea
    c. Over the Andes Mountains in S. America, and
    d. A long band extending east of Japan across the north Pacific Ocean
    e. Additional regions exist just north of the equator in the Atlantic and Indian Oceans and in the oceans around South Africa.

It has long ago been suggested that there may be a link between lightning and solar activity (e.g. Stringfellow, M.F., 1974, Scott et al, 2014). We speculate that the global superbolt data in this paper may give more evidence about this possibility since the sunspot number (see https://www.esrl.noaa.gov/) varies similarly to the upper envelope of the stroke distribution seen in Figure 9. That is, the sunspot number and the envelope of superbolt numbers peak at about the same date (in 2014), and they have a similar broad increase and decrease over these 9 years. We also note that the now well established stroke energy enhancement over oceans (compared to continents) (see Hutchins et al, 2013 or using a different technique, Bierle et al, 2014) is not well explained, and these extreme energy strokes, with their distribution given here, may help in the solution of that problem.

We also know that cosmic rays play an important role in atmospheric electrodynamics (for instance, atmospheric conductivity is provided by the cosmic rays). The question of whether cosmic rays cause or inhibit lightning is an open one, although it may be doubtful there is a direct connection (see Dywer, 2008). We do know, however, that cosmic ray intensity varies inversely with the sunspot cycle, so the temporal stroke envelope variation in Figure 9 could be inversely related to cosmic ray intensity during these times.

We certainly suggest the need for a comprehensive study of the meteorology and dynamics around the thunderstorms near the Andes mountains to address the apparent anomalous seasonal peak in superbolts which occurs there in summer over the western high continental mountains, while most other major superbolt peaks are oceanic and occur in winter weather.

Acknowledgements
The authors wish to thank the World Wide Lightning Location Network (http://wwlln.net), a collaboration among over 50 universities and institutions, for providing the lightning location data used in this paper. In addition the authors thank the Earth Networks for the use of ENTLN lightning location data, and the New Zealand MetService Ltd. for the use of the NZLDN observations, in both cases provided by agreement. The data used in this paper are available from any WWLLN host or may be ordered from links at http://wwlln.net.

References.

Abarca, Sergio F., Kristen L. Corbosiero and Thomas J. Galarneau Jr., An evaluation of the Worldwide Lightning Location Network (WWLLN) using the National Lightning Detection Network (NLDN) as ground truth, JOURNAL OF GEOPHYSICAL RESEARCH, VOL. 115, D18206, doi:10.1029/2009JD013411, 2010

Abreu, D., Chandan, D., Holzworth, R. H., and Strong, K.: A performance assessment of the World Wide Lightning Location Network (WWLLN) via comparison with the Canadian Lightning Detection Network (CLDN), Atmos. Meas. Tech., 3, 1143-1153, https://doi.org/10.5194/amt-3-1143-2010, 2010.

Beirle, S, W. Koshak, R. Blakeslee, and T. Wagner, Global patterns of lightning properties derived by OTD and LIS, Nat. Hazards Earth Syst. Sci., 14, 2715–2726, 2014 doi:10.5194/nhess-14-2715-2014

Burgesser, Rodrigo E., Assessment of the World Wide Lightning Location Network (WWLLN) detection efficiency by comparison to the Lightning Imaging Sensor (LIS), Q. J. R. Meteorol. Soc. 143: 2809–2817, October 2017 A DOI:10.1002/qj.3129

Burkholder, Brian S., Michael L. Hutchins, Michael P. McCarthy, Robert F. Pfaff, and Robert H. Holzworth, Attenuation of lightning-produced sferics in the Earth-ionosphere waveguide and low-latitude ionosphere, J. Geophys. Res., V. 118, 3692-3699,doi:10.1002/jgra.50351, 2013

Connaughton, V., M. S. Briggs, R. H. Holzworth, M. L. Hutchins, G. J. Fishman, C. A. Wilson-Hodge, V. L. Chaplin, P. N. Bhat, J. Greiner, A. von Kienlin, R. M. Kippen, C. A. Meegan, W. S. Paciesas, R. D. Preece, E. Cramer, J. R. Dwyer, and D. M. Smith, Associations between Fermi Gamma-ray Burst Monitor terrestrial gamma ray flashes and sferics from the World Wide Lightning Location Network, JOURNAL OF GEOPHYSICAL RESEARCH, VOL. 115, A12307, doi:10.1029/2010JA015681, 2010

Dowden, R.L., Brundell, J.B.; Rodger, C.J., VLF lightning location by time of group arrival (TOGA) at multiple sites, Journal of Atmospheric and Solar-Terrestrial Physics, v 64, n 7, May 2002, p 817-30

Dwyer, J. R., Do cosmic rays cause lightning? Scientific American, Jan 24, 2008

Hutchins, M.L., R. H. Holzworth, C. J. Rodger and J. B. Brundell, Far field power of lightning strokes as measured by the World Wide Lightning Location Network, JTech (J. Atmos. and Ocean. Tech. (AMS), V.29, 1102-1110, 2012a

Hutchins, M. L., R. H. Holzworth, J. B. Brundell, and C. J. Rodger, Relative Detection Efficiency of the World Wide Lightning Location Network, Radio Science, 2012RS005049, 2012b

Hutchins, M. L., R. H. Holzworth, C. J. Rodger, S. Heckman and J. B. Brundell, WWLLN Absolute Detection Efficiencies, European Geophysical Meeting, 2012c

Hutchins, M.L. R. H. Holzworth, K. S. Virts, J. M. Wallace, and S. Heckman, Radiated VLF energy differences of land and oceanic lightning, Geophysical Research Letters, Vol. 40, 1-5, doi:10.1002/grl.50406, 2013

Jacobson, Abram R. , Robert H. Holzworth, Jeremiah Harlin, Richard L. Dowden, Erin H. Lay, Performance assessment of the World Wide Lightning Location Network (WWLLN), using the Los Alamos Sferic Array (LASA) array as ground-truth, Journal of Atmospheric and Oceanic Technology (AMS), V.23, pp. 1082-92, August 2006

Kirkland, M. W., An examination of superbolt-class lightning events obsereved b y the FORTE satellite. Los Alamos National Laboratory Report LA-UR-99-1685, 1999.

Lay, Erin H., Abram R. Jacobson, Robert H. Holzworth, Craig J. Rodger, Richard L. Dowden Local Time Variation in Land/Ocean Lightning Count Rates as Measured by the World Wide Lightning Location Network, , J. Geophys. Res. , Vol. 112, D13111, doi:10.1029/2006JD007944, 2007

Price, Colin, Yoav Yair, and Mustafa Asfur, East African lightning as a precursor of Atlantic hurricane activity, , Geophys. Res. Lett., Vol. 34, L09805, doi:10.1029/2006GL028884, 2007

Rodger, Craig J., Simon Werner, James B. Brundell, Erin H. Lay, Neil R. Thomson, Robert H. Holzworth, Richard L. Dowden Detection efficiency of the VLF World-Wide Lightning Location Network (WWLLN): Initial case study, Ann. Geophys., 24, 3197–3214, 2006

Rudlosky, Scott D. and Dustin T. Shea Evaluating WWLLN performance relative to TRMM/LIS, Geophysical Research Letters, Volume 40, Issue 10, 02 April 2013 https://doi.org/10.1002/grl.50428

Scott, C. J., R G Harrison, M J Owens, M Lockwood and L Barnard, Evidence for solar wind modulation of lightning, *Environmental Research Letters, 9* 055004, 2014.

Stringfellow, M. F., Lightning incidence in Britan and the solar cycle, Nature 249,332-333, 1974

Thomson, N. R. (2010), Daytime tropical D region parameters from short path VLF phase and amplitude, J. Geophys. Res., 115, A09313, doi:10.1029/2010JA015355

Thornton, J. A., K. S. Virts, R. H. Holzworth, and T. P. Mitchell (2017), Lightning enhancement over major oceanic shipping lanes, Geophys. Res. Lett, 44, 9102–9111, doi:10.1002/2017GL074982

Turman, JGR 1977

Virts, Katrina S., John M. Wallace, Michaale L. Hutchins, and Robert H. Holzworth, A new ground-based, hourly global lightning climatology, BAMS (AMS), pp.1831-91, Sept 2013, (DOI 10.1175/BAMS-D-12-00082)

Table 1: Annual Global total of WWLLN strokes

Year	Total Yearly WWLLN Strokes	Percent of Previous Year
2010	139	100%
2011	153	110%
2012	189	123%
2013	210	111%
2014	228	108%
2015	225	99%
2016	212	94%
2017	208	98%
2018	233	112%

Table 2: Stroke by stroke comparison of matched Superbolts in CONUS

NETWK	YearMoDa	Hr	Mn	Sec	Lat	Lon	EN:Peak WW:	Current Energy
EN	20130728	8	26	6.13	23.41	-103.41	-242381	Amps
WW	20130728	8	26	6.13	23.52	-103.45	1198810	Joules
EN	20131026	0	52	32.98	34.85	-105.284	-160546	Amps
WW	20131026	0	52	32.98	34.89	-105.37	2063466	Joules
EN	20131105	10	37	25.76	37.64	-100.396	-170516	Amps
WW	20131105	10	37	25.76	37.68	-100.43	1608984	Joules
EN	20131110	10	6	54.73	37.11	-143.977	437788	Amps
WW	20131110	10	6	54.73	37.10	-144.11	1033990	Joules
EN	20131120	7	49	31.32	39.88	-96.1878	-162462	Amps
WW	20131120	7	49	31.32	39.95	-96.21	1707175	Joules
EN	20131122	3	38	25.67	32.63	-96.8329	-285800	Amps
WW	20131122	3	38	25.67	32.66	-96.87	1598585	Joules
EN	20140112	0	59	35.28	36.89	-81.3841	164300	Amps
WW	20140112	0	59	35.28	36.90	-81.37	1326023	Joules
EN	20140112	13	16	21.46	22.43	-102.907	-216616	Amps
WW	20140112	13	16	21.46	22.43	-102.91	1108757	Joules
EN	20140112	13	56	23.92	21.74	-103.403	-294699	Amps
WW	20140112	13	56	23.92	21.74	-103.41	1933439	Joules
EN	20140112	17	38	8.44	22.21	-103.348	-263639	Amps
WW	20140112	17	38	8.44	22.19	-103.34	1989755	Joules
EN	20140112	18	33	9.48	22.91	-102.246	205509	Amps
WW	20140112	18	33	9.48	22.97	-102.28	1233867	Joules
EN	20140112	19	38	29.79	22.46	-103.276	241548	Amps
WW	20140112	19	38	29.79	22.60	-103.3	3371049	Joules
EN	20150107	23	26	24.45	23.02	-104.319	-261997	Amps
WW	20150107	23	26	24.45	22.98	-104.35	1006988	Joules
EN	20150109	7	49	49.57	27.72	-107.245	-245496	Amps
WW	20150109	7	49	49.57	27.77	-107.29	2744531	Joules
EN	20151210	6	16	30.17	41.71	-132.57	-393140	Amps
WW	20151210	6	16	30.17	41.74	-132.55	1079403	Joules
EN	20160202	2	1	51.82	35.85	-99.8	-245654	Amps
WW	20160202	2	1	51.82	35.89	-99.4	1331675	Joules
EN	20160307	4	50	32.13	40.10	-134.4	567009	Amps
WW	20160307	4	50	32.13	40.10	-134.41	1333542	Joules
EN	20170115	8	0	52.12	36.11	-102.8	-235222	Amps
WW	20170115	8	0	52.12	36.20	-102.76	2076322	Joules

519 Figures:

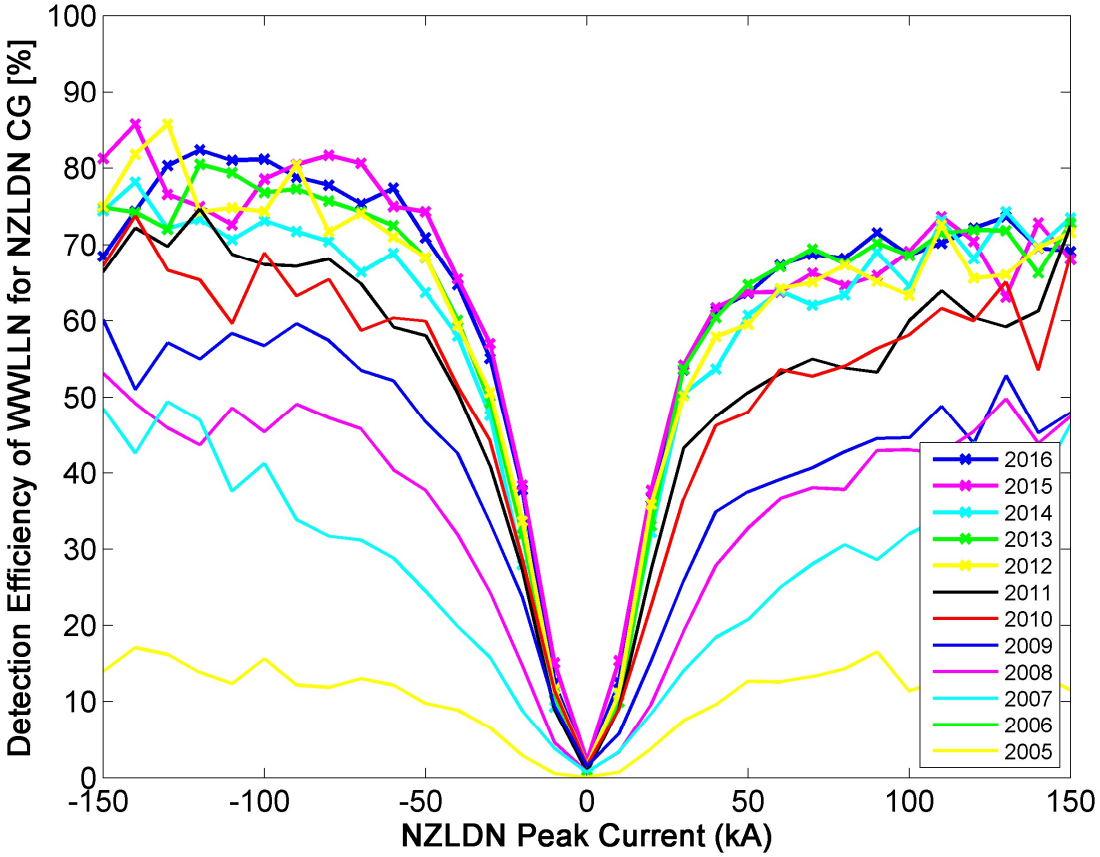

520
521 Figure 1. WWLLN lightning stroke detection efficiency by comparison to the New Zealand
522 Lightning Detection Network (NZLDN) (update of Fig 5 of Rodger et al, 2006)

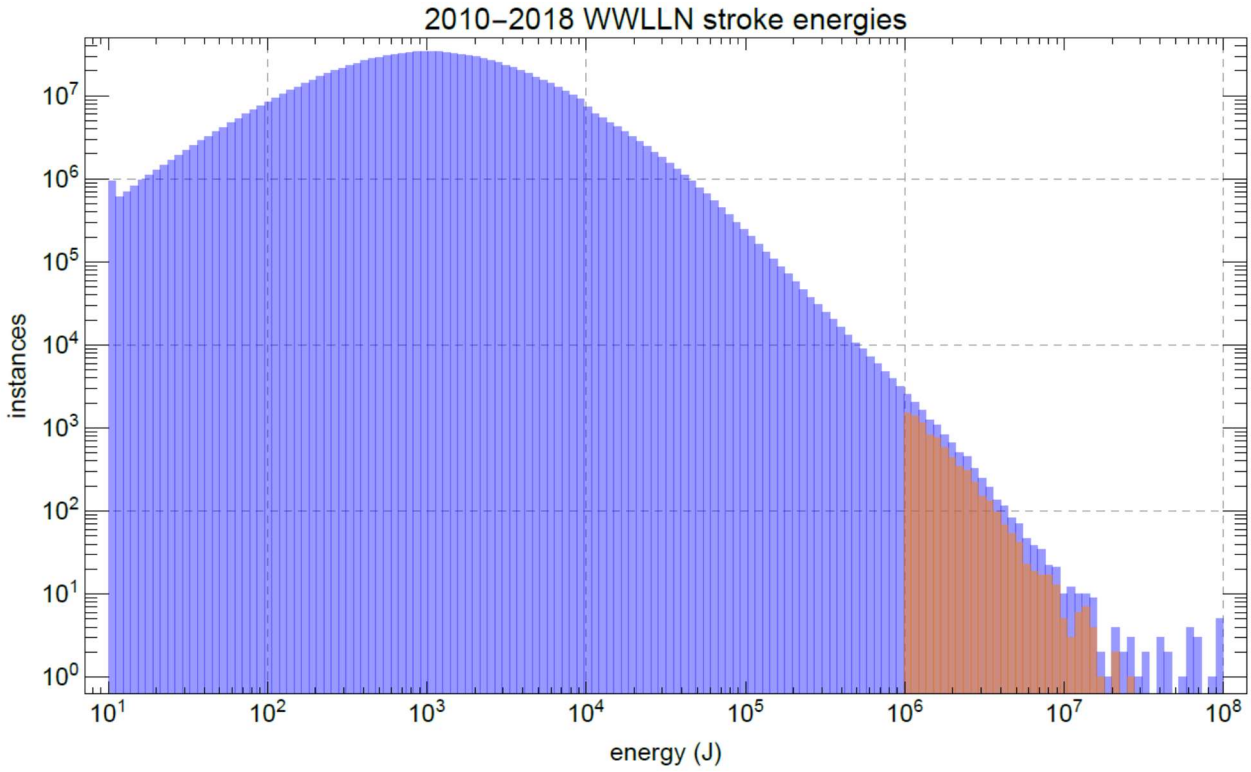

Figure 2. Distribution of stroke energies for WWLLN data set including the nine years 2010 – 2018 (blue). The brown colored distribution above 10^6 J presents the distribution we call superbolts with stroke energies more than 3 orders of magnitude above the mean and median of the total distribution. One can see this is a natural continuation of the total distribution, with a small reduction to ensure the analysis is done only on well located strokes, with relatively small standard error in the energy/stroke calculations.

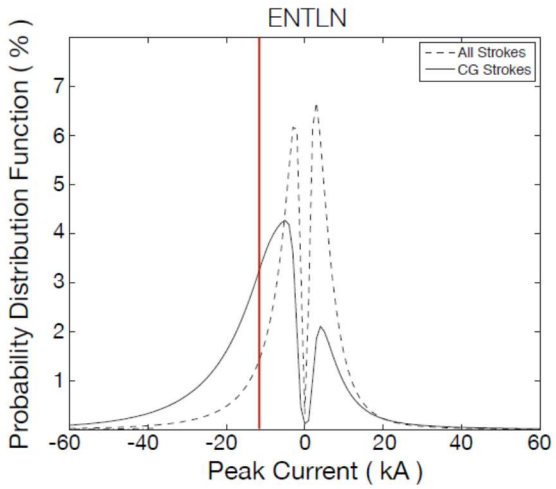

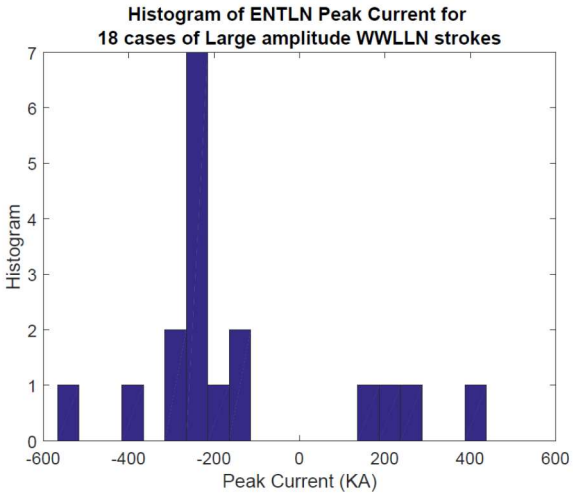

551 Figure 3a. ENTLN peak current distribution
552 for CONUS in 2011 (from Hutchins et al,2012c)
553 showing the mean -CG current of -13 kA (red)
554
555

Figure 3b. ENTLN peak current for 18 matched WWLLN large energy strokes Mean –CG current = -267 kA (from Table 2)

556

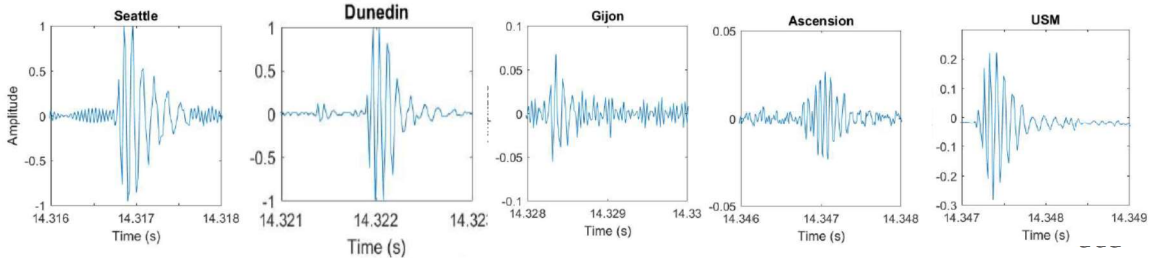

564

565 Figure 4. Large Amplitude stroke Waveform Sample at 2019/01/17 23:16:14 UTC
566 These five panels show the quality of the received waveforms at 5 WWLLN stations separated by up to
567 16,666 km from the stroke. Each station has differing noise backgrounds and different electronic gains.
568 The amplitudes are in normalized sound card units for each station. Station distances from the stroke
569 (in parentheses), and TOGA times in UTC seconds after the stroke time (2019/01/17 23:16:14 UTC) are:
570 Seattle (7594.2 km) 14.3168 s, Dunedin (9123.12 km) at 14.322 s, Gijon (11001 km) at 14.3283
571 s, Ascension (16487.8 km) at 14.3467 s, and USM (16666.9 km) at 14.3473 s.
572
573
574
575
576
577
578
579
580

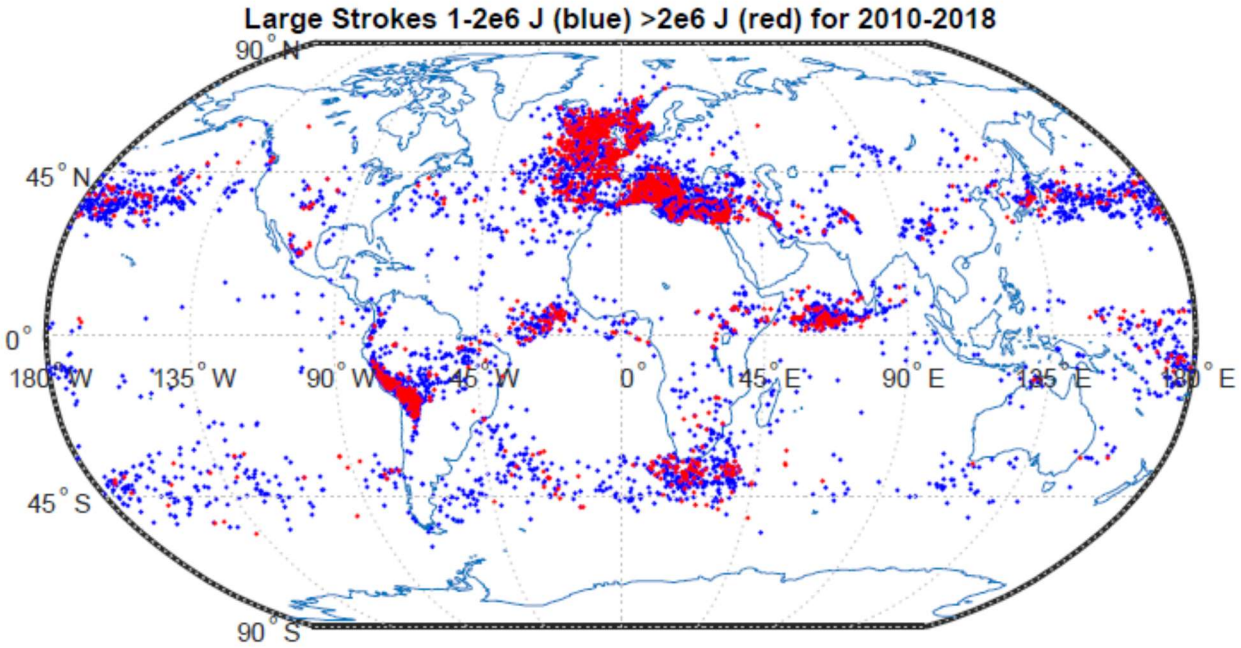

Figure 5: Global distribution of all superbolts, with 1-2e^6 J (blue) and >2e^6 J (red)

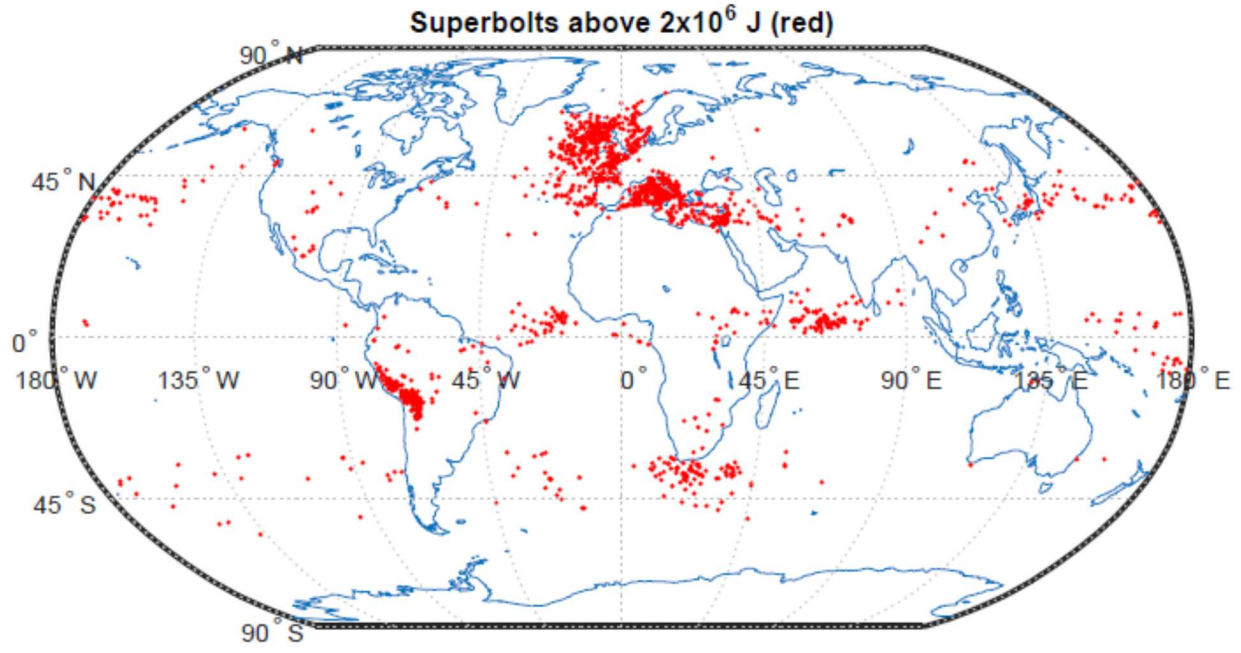

Figure 6: Same as Figure 5 with just superbolts having energies > 2e^6 J (red)

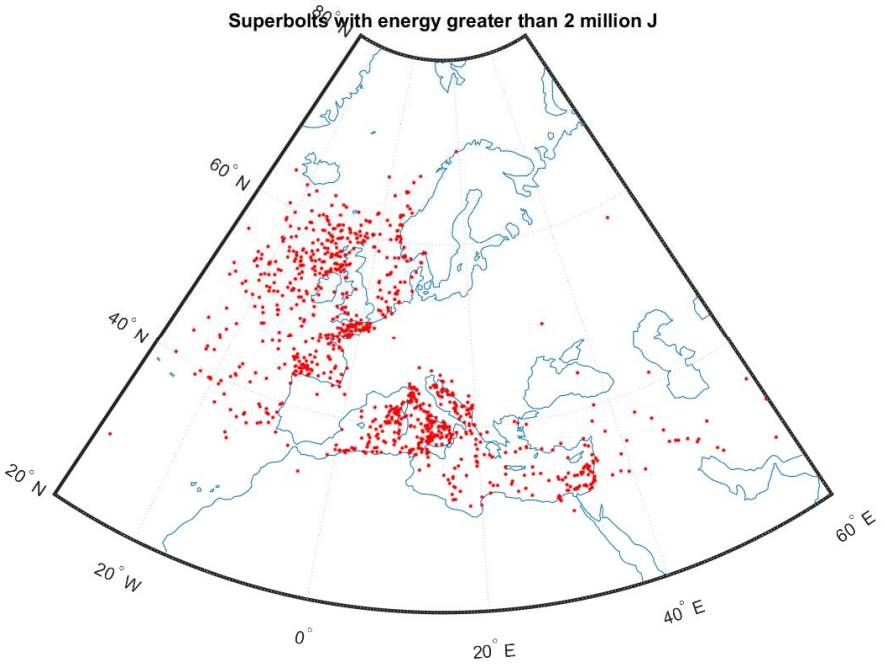

Figure 7. – same as Figure 6 but zooming in on Europe

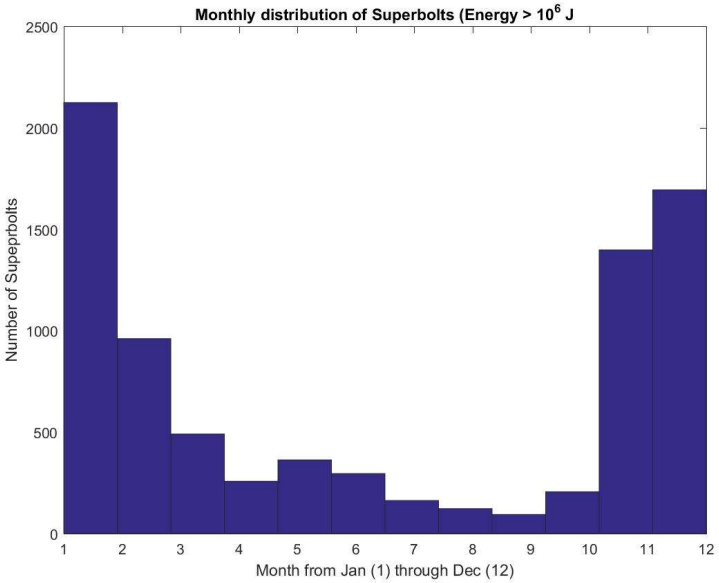

Figure 8: Monthly distribution of all Superbolts

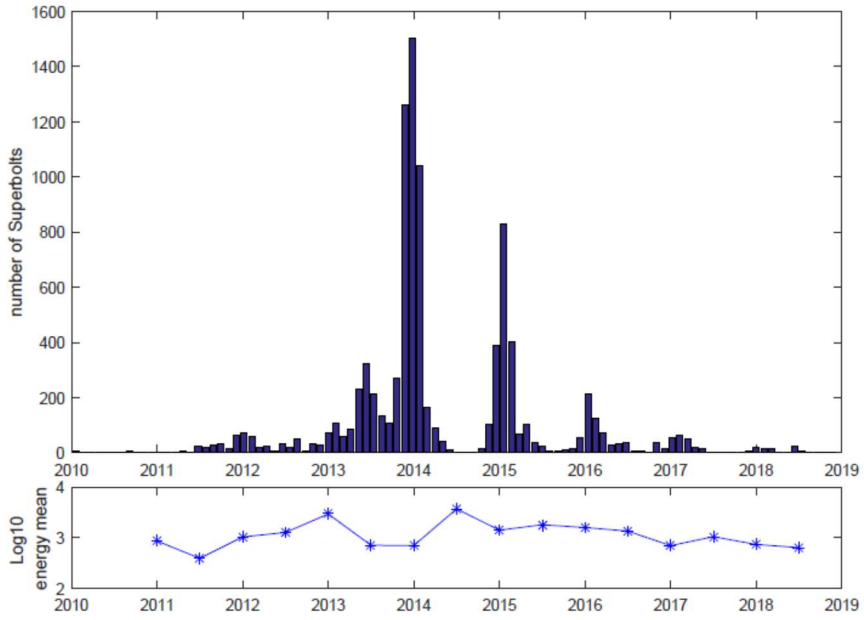

Figure 9. Histogram of the monthly total of the largest Superbolts and a plot of The log10 of the mean energy for all WWLLN strokes by winter and summer season, using Dec-Jan and June-July each year. (e.g. mean energy for all WWLLN is about 1000 J = 3.0 in log10 space).

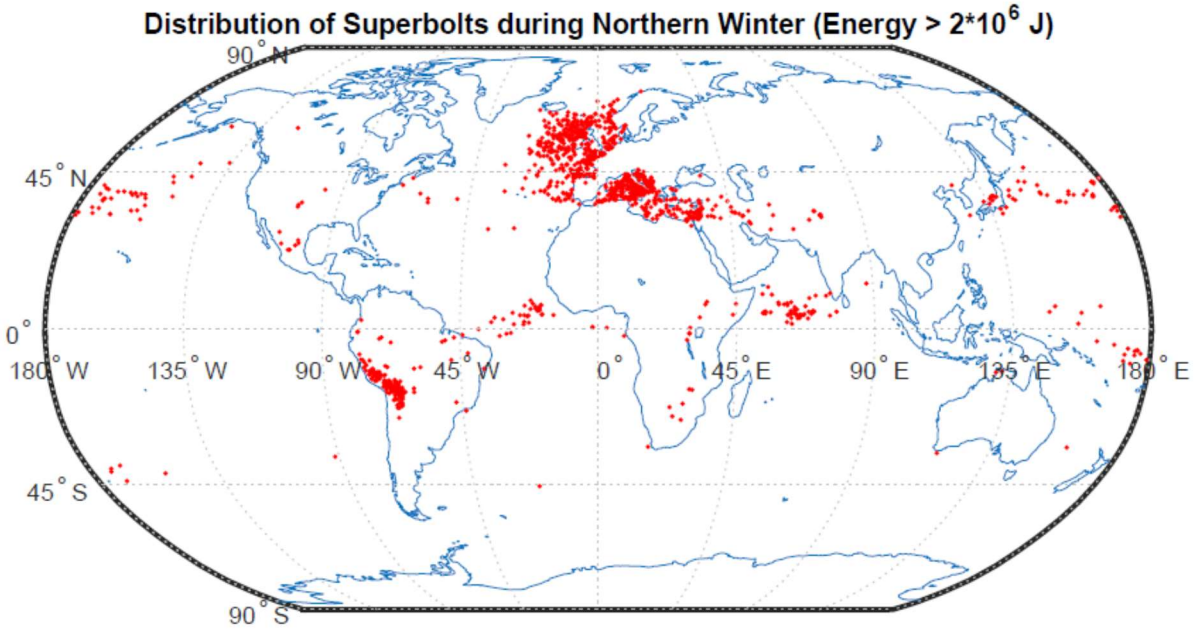

Figure 10: Global Distribution of Superbolts using just strokes in Nov, Dec, Jan and Feb 2010-2018 with energy $>2*10^6$ J